Point defect induced degradation of electrical properties of Ga_2O_3 by 10 MeV proton damage

A. Y. Polyakov, N. B. Smirnov, I. V. Shchemerov, E. B. Yakimov, Jiancheng Yang, F. Ren, Gwangseok Yang, Jihyun Kim, A. Kuramata, and S. J. Pearton

Citation: Appl. Phys. Lett. **112**, 032107 (2018);
View online: https://doi.org/10.1063/1.5012993
View Table of Contents: http://aip.scitation.org/toc/apl/112/3
Published by the American Institute of Physics

Point defect induced degradation of electrical properties of Ga_2O_3 by 10 MeV proton damage

A. Y. Polyakov,[1] N. B. Smirnov,[1] I. V. Shchemerov,[1] E. B. Yakimov,[1,2] Jiancheng Yang,[3] F. Ren,[3] Gwangseok Yang,[4] Jihyun Kim,[4] A. Kuramata,[5] and S. J. Pearton[6]
[1]*National University of Science and Technology MISiS, Moscow 194017, 4 Leninsky Ave., Russia*
[2]*Russia and Institute of Microelectronics Technology and High Purity Materials, Russian Academy of Science, 6, Academician Ossipyan str., Chernogolovka, Moscow Region 142432, Russia*
[3]*Department of Chemical Engineering, University of Florida, Gainesville, Florida 32611, USA*
[4]*Department of Chemical and Biological Engineering, Korea University, Seoul 136-713, South Korea*
[5]*Tamura Corporation and Novel Crystal Technology, Inc., Sayama Saitama 350-1328, Japan*
[6]*Department of Materials Science and Engineering, University of Florida, Gainesville, Florida 32611, USA*

(Received 9 November 2017; accepted 5 January 2018; published online 17 January 2018)

Deep electron and hole traps in 10 MeV proton irradiated high-quality β-Ga_2O_3 films grown by Hydride Vapor Phase Epitaxy (HVPE) on bulk β-Ga_2O_3 substrates were measured by deep level transient spectroscopy with electrical and optical injection, capacitance-voltage profiling in the dark and under monochromatic irradiation, and also electron beam induced current. Proton irradiation caused the diffusion length of charge carriers to decrease from 350–380 μm in unirradiated samples to 190 μm for a fluence of 10^{14} cm^{-2}, and this was correlated with an increase in density of hole traps with optical ionization threshold energy near 2.3 eV. These defects most likely determine the recombination lifetime in HVPE β-Ga_2O_3 epilayers. Electron traps at E_c-0.75 eV and E_c-1.2 eV present in as-grown samples increase in the concentration after irradiation and suggest that these centers involve native point defects. *Published by AIP Publishing.*
https://doi.org/10.1063/1.5012993

β-Ga_2O_3 is attracting attention because of its combination of physical properties that are attractive for high-power electronics and solar-blind UV photodetectors.[1–4] The bandgap of this transparent oxide is close to 4.85 eV, the electrical breakdown field is very high, 8 MV/cm compared to 2.5 MV/cm in SiC and 3.3 MV/cm in GaN, while the saturation velocity of electrons of 2×10^7 cm/s is as high as in SiC and only slightly lower than that in GaN.[1–6] The material can be grown with high crystalline quality in bulk form by various versions of solution growth, and high quality epitaxial growth on native Ga_2O_3 substrates, on Si, or on sapphire can be achieved.[4–8] N-type doping is controllable both in bulk crystals and in epitaxial films. Large area substrates are commercially available, and a number of different devices such as Schottky rectifiers, metal and oxide-gate transistors, and photodetectors have been reported.[9–14] Theoretical and experimental work aimed at understanding the nature of donor dopants, the type of dominant deep traps, and the effects of irradiation and surface damage is also increasing.[15–22] Theory predicts Si and Sn to be efficient shallow donors and oxygen vacancies to be deep double donors.[15] Deep level transient spectroscopy (DLTS) and deep level optical spectroscopy (DLOS) have observed three major electron traps with levels near E_c-(0.5–0.6) eV, E_c-(0.7–0.8) eV, and E_c-1 eV[17] and two hole traps with levels near E_c-2.2 eV and E_c-4.4 eV in bulk β-Ga_2O_3.[17] Korhonen *et al.*[18] investigated the electrical compensation in n-type Ga_2O_3 by Ga vacancies using positron annihilation spectroscopy and estimated a V_{Ga} concentration of at least 5×10^{18} cm^{-3} in their undoped and Si-doped samples. Since theoretical calculations predict that these V_{Ga} values should be in a negative charge state for n-type samples, they will compensate *n*-type doping. Kananen *et al.*[19] used electron paramagnetic resonance to demonstrate the presence of both doubly ionized (V_{Ga}^{2-}) and singly ionized (V_{Ga}^{-}) acceptors at room temperature in bulk Ga_2O_3.

In terms of radiation damage, electron irradiation has been shown to increase the resistivity of the epitaxial material, decrease the diffusion length of nonequilibrium charge carriers, and increase leakage current and decrease the breakdown voltage of rectifiers made on epitaxial β-Ga_2O_3.[21–24] Weiser *et al.*[20] showed that the dominant defect created in the proton-irradiated material is particularly the Ga vacancy decorated by two hydrogens. Arehart *et al.*[22] reported a trap at Ec-1.88 eV in neutron irradiated diodes. However, little is known about the deep trap spectra and the types of centers that contribute to nonradiative recombination in high-quality epitaxial materials irradiated with protons. In this letter, we present a study of deep trap spectra and diffusion length measurements performed on high-quality β-Ga_2O_3 films before and after irradiation with 10 MeV protons and discuss which defects can be held responsible for the observed compensation of the material and the decrease of the diffusion length induced by irradiation.

The epitaxial β-Ga_2O_3 films were grown by hydride vapor phase epitaxy (HVPE) on β-Ga_2O_3 substrates from bulk edge-defined film-fed (EFG) crystals. The substrates had (001) orientation and a thickness of 650 μm and were n-type doped by Sn to a donor concentration of 3.6×10^{18} cm^{-3}. The HVPE films had an initial thickness of 20 μm and were lightly doped with Si. After the growth, the films were chemically mechanically polished down to a final thickness of about 10 μm to remove surface pits and planarize the surface.[21,24] The half-width of the (402) x-ray diffraction peak (triple axis

arrangement) was ~10 arc sec, and the dislocation density determined by etch pit counting and by electron beam induced current (EBIC) imaging was on the order of 10^3 cm^{-2}.

Schottky diodes were prepared by lift-off of E-beam evaporation of Ni/Au on the film side. The diameter of the Schottky diodes was 0.51 mm. The Ohmic contacts to the substrate side were made by Ti/Au deposition. The samples were irradiated with 10 MeV protons with a fluence of 10^{14} cm^{-2} in a linear proton accelerator of Korea University. Before and after irradiation, the current-voltage (I-V), capacitance-voltage (C-V), admittance spectra,[25,26] electrical (DLTS), and optical (ODLTS)[27,28] measurements were performed in the temperature range of 85–400 K using an Oxford Instruments gas-flow cryostat and in the range of 300 K–500 K on a custom-built hot stage. The samples were also characterized by electron beam induced current (EBIC) and microcathodoluminescence (MCL).[27–30] From the EBIC collection efficiency dependence on accelerating voltage of the electron probe beam, the value of diffusion length L_d was calculated.[29,30] Multiple samples of each type were examined, and we report the range of concentrations observed.

The β-Ga_2O_3 epi had a net donor concentration N_d of ~3.8×10^{16} cm^{-3} as determined by C-V measurements. The Ni barrier height derived from the voltage intercept in the $1/C^2$ versus voltage plot was ~1.1 eV.[31] The I-V showed an ideality factor of 1.1 and an activation energy of the saturation current (corrected for temperature T by dividing by $T^{3/2}$) of ~0.9 eV. For lower temperatures, the temperature dependence weakened and the ideality factor increased, suggesting a growing contribution of thermally enhanced tunneling. After the irradiation with a proton fluence of 10^{14} cm^{-2}, the net donor concentration decreased to 2.5×10^{15} cm^{-3} and the barrier height slightly increased to 1.2 eV.

DLTS spectra measurements showed the presence of a prominent peak corresponding to electron trap near E_c-1.05 eV and the apparent electron capture cross section of $\sigma_n = 2 \times 10^{-12}$ cm^2 [Fig. 1(a)]. Two minor traps with levels E_c-0.6 eV ($\sigma_n = 5.6 \times 10^{-15}$ cm^2) and E_c-0.75 eV ($\sigma_n = 6.5 \times 10^{-15}$ cm^2) were also detected. No other electron trap peaks were observed up to the measurement temperatures of 500 K. After proton irradiation, the dominant peak in DLTS spectra was an electron trap with level E_c-0.75 eV (electron capture cross section $\sigma_n = 6.5 \times 10^{-15}$ cm^2) and with a prominent shoulder due to the E_c-1.05 eV electron trap [Fig. 1(a)]. The signal from the minor traps at E_c-0.6 eV might still have been present but may have been masked by the E_c-0.75 eV peak. At higher temperature, we also observed an electron trap with level E_c-1.2 eV and an electron capture cross section of 5.4×10^{-15} cm^2 [high-temperature portion of the spectra in Fig. 2(b)]. This trap was not detected in control samples. The y-ordinate in Fig. 1 is the DLTS correlator signal ΔC divided by the steady-state capacitance C ($\Delta C/C$) and multiplied by $2N_d$ and by the DLTS spectrometer correlator function F^{-1}.[26] At peaks in the spectra, the magnitude corresponds to the trap concentrations but uncorrected for the fact that the DLTS signal does not come from the entire space charge region but only from the part of this region where the trap occupation changes when the forward bias pulse is applied. The actual trap concentrations were corrected using the standard λ-correction procedure taking into account the quiescent bias and forward bias pulses used (−2 V and +1 V,

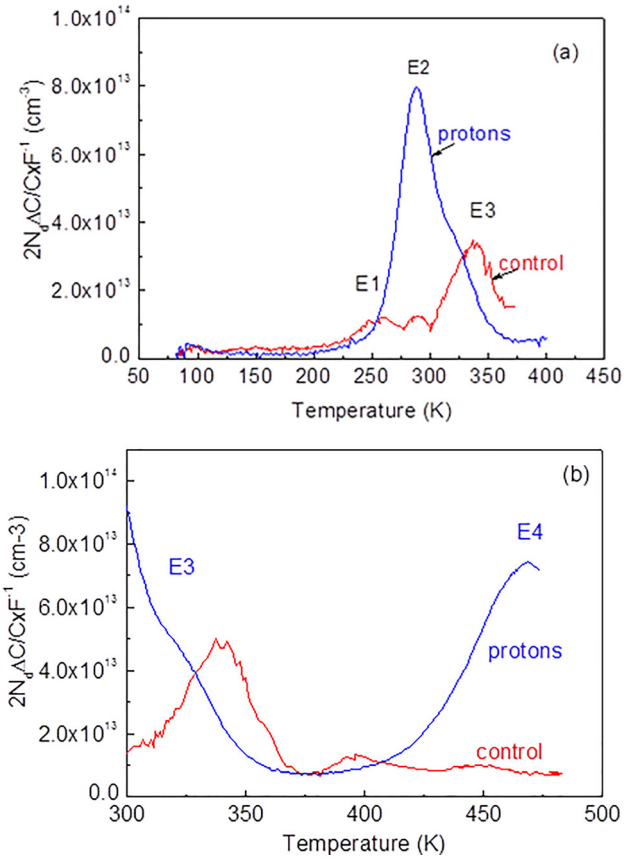

FIG. 1. (a) DLTS spectra for β-Ga_2O_3 epilayers, bias −2 V, bias pulse +1 V, time windows 1.75 s/17.5 s; (b) high temperature part of the DLTS spectra, bias −2 V, pulse +1 V, and time windows 1.75 ms/17.5 ms before (red line) and after (blue line) proton irradiation.

respectively).[26,31] These trap concentrations are shown in Table I. The E_c-0.6 eV, E_c-0.75 eV, and E_c-1.05 eV electron traps are similar to the electron traps observed in DLTS spectra of Czochralski-grown[16] or EFG[17] β-Ga_2O_3 crystals. In the notation of Ref. 16, these are E1, E2, and E3 electron traps, respectively. The concentrations of all the electron traps in the epitaxial films used here are 1–2 orders of magnitude lower than that in bulk β-Ga_2O_3. The concentrations of E2 and E3 increased, and new traps E4 at E_c-1.2 eV emerged after proton

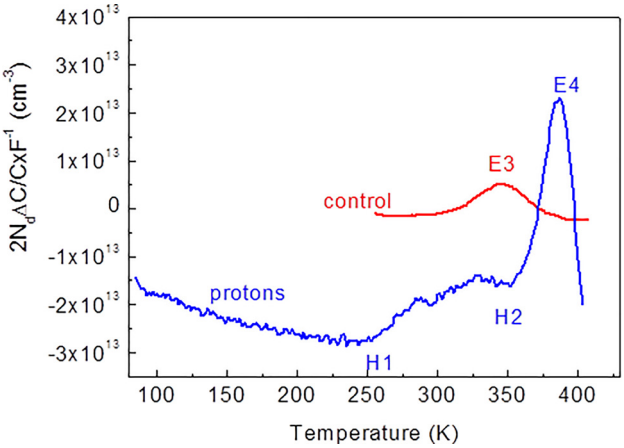

FIG. 2. ODLTS spectra before (red line) and after (blue line) proton irradiation; excitation with high-power 3.4 eV LED, bias −2 V, time windows 1 s/3 s for reference, and 8.25 s/24.75 s for sample after proton irradiation.

TABLE I. Deep traps detected in β-Ga_2O_3 epilayers.

	Trap concentration (cm^{-3})					
Sample	E1(E_c-0.6 eV)	E2 (E_c-0.75 eV)	E3 (E_c-1.05 eV)	E4 (E_c-1.2 eV)	E_c-2.3 eV	L_d (μm)
Control	3.6×10^{13}	4.6×10^{13}	1.1×10^{14}	…	1.25×10^{15}	350
Proton irradiated	…	3.2×10^{14}	2.3×10^{14}	4.5×10^{14}	2.3×10^{15}	190

irradiation. The presence of deeper electron traps could not be probed by DLTS because the respective peak temperatures are too high to be detected in our setup even for long time windows (restricting detection to trap energies lower than 1.3 eV from the conduction band edge) and because it is difficult to recharge traps deeper than ~1.1 eV (the estimated Schottky barrier height) by majority carrier injection pulse.[26]

The presence of hole traps in the lower half of the bandgap was probed by ODLTS, allowing recharging of both electron and hole traps through optical injection. As in DLTS, the probed energy interval is restricted to ~1.3 eV region from the conduction and valence band edges. For samples before irradiation, only the E3 traps were observed (Fig. 2). After proton irradiation, we observed a very broad low temperature hole trap band with an activation energy of 0.4 eV (H1 trap in Fig. 2), a hole trap peak with level near $E_v + 1.2$ eV (H2 trap), and the E4 electron trap. The concentrations in Fig. 2 are calculated from $2N_d$ ($\Delta C/C$) F^{-1} but do not take into account the actual width of the space charge region where the traps are recharged by the light injection pulse because of existing uncertainties in the relevant absorption coefficient value. Injection was accomplished with a high-power light emitting diode (LED) with a photon energy of 3.4 eV. This photon energy is too low to directly excite hole traps near $E_v + 0.4$ eV, and the excitation could only be from the valence band tails or by two-photon absorption and thus inefficient; so, the shallow hole trap concentration is underestimated.

A comment is appropriate here as to the measurement of hole trap transients. Theory predicts that in β-Ga_2O_3, holes can form self-trapped hole (STH) polaronic states with very low mobility.[32] Electron excitation from deep traps in the lower half of the bandgap will produce holes on these traps, which are clearly emitted at elevated temperatures into the valence band. If the STHs are not mobile and do not leave the space charge region (SCR), the charge and capacitance would not change with time. The electron trap, ET3, in the ODLTS spectrum appears because electrons in the valence band are excited during the light pulse into the partly occupied ET3 traps, very close to the Fermi level whose position is determined by the Schottky barrier height. The trapped electrons are then re-emitted into the conduction band after the end of the pulse. However, if the holes are not mobile and the optically generated holes in the valence band cannot be swept out of the SCR during the excitation pulse, the non-equilibrium charge would not be formed and the electron trap feature in ODLTS similar to the feature in DLTS would not be observed. The fact that such features are observed in ODLTS is an indication that holes in β-Ga_2O_3 are not as immobile as predicted by theory. Recent studies do indeed suggest that holes could be mobile in β-Ga_2O_3 although the gallium vacancy acceptors supplying them, V_{Ga}, are deep, with the ionization energy of 1.2 eV.[33] Interestingly, our H2 hole traps have a similar energy level.

Deeper electron and hole traps not accessible by DLTS/ODLTS measurements can be detected by photocapacitance spectra and by C-V profiling under illumination [light C-V (LCV)] with various photon energies.[34] We carried out these measurements using a set of high-power LEDs with photon energies in the range of 1.3–3.4 eV. For each photon energy, the power of the LED was set to reach the signal saturation in LCV. These spectra (the concentration under illumination minus dark concentration) are shown in Fig. 3. All spectra show a prominent optical threshold near 2.3 eV similar to the optical threshold of the Ec-2.16 eV hole traps in DLOS spectra of bulk EFG β-Ga_2O_3.[22] The concentration was determined in the near-plateau region in the LCV spectra. The measurements were performed with a slow voltage sweep to make sure that the quasi-equilibrium has been reached. The main uncertainty in this estimate of the concentration comes from the uncertainty in the relative values of the optical cross sections for holes and electrons.

Do the observed deep electron or hole traps control recombination of excess charge carriers in β-Ga_2O_3? The diffusion lengths L_d of nonequilibrium charge carriers in the Schottky diodes were calculated from the measured EBIC current I(EBIC) collection efficiency dependence on the SEM probing beam acceleration voltage E_b. The experimental dependence in Fig. 4 was then fitted to a model involving the depth distribution of the electron-hole pairs as a function of energy E_b and current I_b. The losses in collection efficiency come from charge carrier recombination in the quasi-neutral region, described by the ambipolar diffusion length L_d and by absorption in the Schottky metal. The fitting parameters in the model are thus L_d, the metal thickness, and the width of the space charge region determined by the

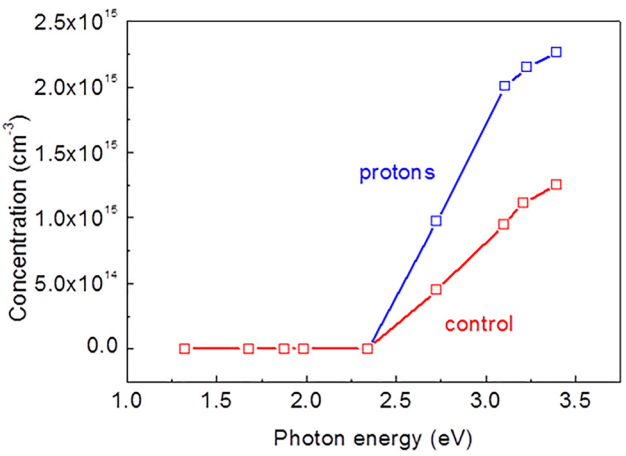

FIG. 3. LCV spectra for β-Ga_2O_3 epilayers before (red squares) and after (blue squares) proton irradiation.

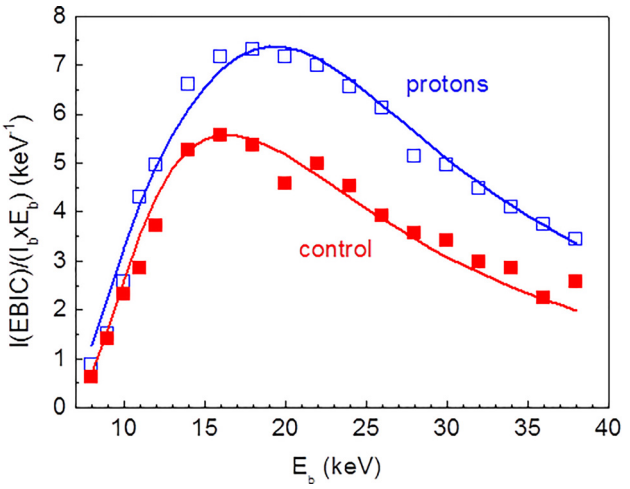

FIG. 4. EBIC current collection efficiency as a function of accelerating voltage of SEM probe beam before (red) and after (blue) proton irradiation (squares are experimental points, solid lines are the result of fitting). The diffusion lengths are 350 nm for the control and 190 nm after proton irradiation.

concentration of uncompensated donors N_d.[29] The advantage of this approach compared to scanning the SEM beam along the surface of the sample and monitoring the decrease in the EBIC current as a function of the distance of the probing beam to the Schottky barrier edge[29] is that the calculated diffusion lengths values do not depend on the surface recombination velocity and on the probing beam accelerating voltage (i.e., excitation depth).[29] The disadvantage is that the charge carrier generation function has to be calculated (by Monte Carlo modeling[29]) and there is no simple analytical procedure to extract the L_d values from the measured charge collection efficiency. The calculated values of L_d are presented in Table I.

The question arises as to whether the holes are mobile in β-Ga_2O_3? The standard situation is that electrons and holes are created by the electron probing beam in the SCR and in the quasi-neutral part of the Schottky diode. The excess carriers outside the SCR are taken to the SCR edge via ambipolar diffusion, electrons and holes are separated, and the holes are carried by the SCR electric field to the Schottky diode metal. If the holes are not mobile, this mechanism does not apply and we should not see the EBIC signal, particularly when the probing beam is placed far away from the Schottky diode edge. By contrast, we see that EBIC current is at least two orders of magnitude higher than the current of the probing beam which was close to 0.1 nA. The EBIC signal has the "correct" sign expected when holes are carried through the space charge region. This occurs even when the probing beam is placed far away from the diode edge. Since our EBIC measurements are performed in the photovoltaic mode (no bias on the diode), photoconductivity due to electrons is not present, and in addition, the injection level in our experiment was low. It has been proposed that, with strong intrinsic light excitation, STHs formed very near to the Schottky metal can decrease the barrier height and increase the diode reverse current,[35] but such a mechanism does not explain the large magnitude of the EBIC current compared to the beam current when the excitation is done far away from the edge of the diode. Once again, our experimental data imply that holes in β-Ga_2O_3 can indeed be mobile.

If the recombination is determined by deep traps, one can estimate possible roles of different centers detected in DLTS, ODLTS, and LCV by comparing the results with diffusion lengths values. These diffusion lengths are related to ambipolar mobility through $L_d = (\tau \mu k_B T/e)^{1/2}$, where $\tau = (\sigma v_{th} N_t)$ is the recombination lifetime determined by the presence of deep traps, μ-the ambipolar mobility, k_B the Boltzmann constant, e the electronic charge, σ the capture cross section, v_{th} the thermal velocity of charge carriers, and N_t the concentration of deep traps-recombination centers.[29] Thus, the values of L_d^2 give the range of changes of the $\mu\tau$ product from sample to sample and, if the mobility changes are not strong, suggest the relative changes of the density of recombination centers. From Table I, we see that the ET2, ET3, and E_c-2.3 eV trap concentrations increase after irradiation, and thus, these traps are potential lifetime killers. In addition, one has to consider the ET4 electron traps and the H2 hole traps appearing in relatively high densities after proton irradiation. Some additional measurements allow us to narrow down the circle of candidates. For example, Table I gives the concentrations of deep traps in one of the studied samples before irradiation. In other samples, the measured net donor concentration could be much lower, 3×10^{15} cm^{-3}. The ET1, ET2, and E_c-2.3 eV concentrations in this sample were very close to the ones in our reference sample in Table I, 2.1×10^{13}, 5.6×10^{13}, and 8.5×10^{14} cm^{-3}, respectively. The concentration of the ET3 traps was virtually the same as in the irradiated sample and twice as high as for the reference sample, 2.1×10^{14} cm^{-3}. No ET4 traps or H2 traps could be detected. The L_d value in this sample was 380 nm, even higher than for the reference sample. This indicates that the ET3 traps are not our lifetime killers.

The ET2 trap also seems not to be a good candidate. The DLTS peak magnitude of ET2 in the irradiated sample showed a dependence on the injection pulse length. Measurements of the temperature dependence of the capture cross section[31] gave the electron capture cross section temperature dependence as $\sigma_n = 1.3 \times 10^{-16} \exp(-0.36/k_B T)$ with a relatively high barrier for capture of electrons, which is not a good feature for a proper lifetime killer. Thus, we are left with the E_c-2.3 eV traps and possibly the ET4 electron traps and H2 hole traps as possible candidates.

Regarding the nature of the observed electron and hole traps, it has been suggested that the E1, E2, and E3 electron traps could be associated with transition metal impurities.[16] However, at least for the E2 traps, their concentration increased after irradiation, indicating the traps to be complexes involving native defects. It is also not clear where the Ga vacancy-2H complex has a level in the gap. The energy levels of the major electron and hole traps near E_c-1.2 eV (E4) and E_c-2.3 eV in irradiated β-Ga_2O_3 are not too far from the charge transfer levels of two types of oxygen vacancies predicted by theory.[15] As mentioned above, the level of H2 traps is close to the level attributed to Ga vacancy acceptors.[33]

Finally, the question arises as to the defects responsible for the strong donor compensation after proton irradiation. None of the defects in Table I has the required concentration and we assume that the compensating radiation defects have levels relatively close to the valence band in the region not accessed by DLTS, ODLTS, and LCV measurements.

Defects of such sort with levels near $E_v + 0.4$ eV have been observed by DLOS in bulk β-Ga_2O_3 at high concentrations.[16,22] We see features in ODLTS of the proton irradiated sample that could be attributed to similar defects, the traps giving rise to the broad H1 ($E_v + 0.4$) eV feature in Fig. 3, but our shortest wavelength excitation LED source with a photon energy of 3.4 eV was inefficient in recharging these traps, which explains their apparently low concentration.

In conclusion, high-quality epitaxial films of β-Ga_2O_3 grown by HVPE on native substrates exhibit deep electron traps having levels near E_c-0.6 eV, E_c-0.75 eV, and E_c-1.05 eV, similar to the E1, E2, and E3 electron traps observed in bulk β-Ga_2O_3 crystals.[16,17] The concentration of these traps in the HVPE films is 1–2 orders of magnitude lower than in the bulk material. The most prominent deep center in the epilayers has an optical excitation threshold near 2.3 eV. These centers are similar to the E_c-2.16 eV trap observed in DLOS and photocapacitance spectra of bulk β-Ga_2O_3.[17] Proton irradiation increases the density of the E2 (E_c-0.75 eV) and E_c-2.3 eV traps, suggesting that these traps incorporate native defects. Changes in ambipolar diffusion lengths as a result of proton irradiation point to the E_c-2.3 eV and possibly the ET4 electron traps and H2 hole traps as likely defects determining the recombination lifetime in HVPE β-Ga_2O_3 epilayers. Our ODLTS and EBIC results are difficult to explain if one assumes that all holes in β-Ga_2O_3 are not mobile polaronic self-trapped hole states.[32]

The work at NUST MISiS was supported in part by the Ministry of Education and Science of the Russian Federation in the framework of Increase Competitiveness Program of NUST «MISiS» (K2-2014-055). The work at UF was sponsored by the Department of the Defense, Defense Threat Reduction Agency, HDTRA1-17-1-011, monitored by Jacob Calkins. The work at Korea University was supported by the Korea Institute of Energy Technology Evaluation and Planning (KETEP), the Ministry of Trade, Industry, and Energy of Korea (No. 20172010104830), and the Space Core Technology Development Program (2017M1A3A3A02015033) through the National Research Foundation of Korea funded by the Ministry of Science, ICT and Future Planning of Korea. The work at Tamura was partially supported by the New Energy and Industrial Technology Development Organization (NEDO), Japan. We also thank Dr. Kohei Sasaki from Tamura Corporation for fruitful discussions.

[1]S. I. Stepanov, V. I. Nikolaev, V. E. Bougrov, and A. E. Romanov, Rev. Adv. Mater. Sci. **44**, 63 (2016), see http://www.ipme.ru/e-journals/RAMS/no_14416/06_14416_stepanov.pdf.
[2]H. von Wenckstern, Adv. Electron Mater. **3**, 1600350 (2017).
[3]M. A. Mastro, A. Kuramata, J. Calkins, J. Kim, F. Ren, and S. J. Pearton, ECS J. Solid State Sci. Technol. **6**, P356 (2017).
[4]S. Rafique, L. Han, and H. Zhao, ECS Trans. **80**, 203 (2017).
[5]D. Gogova, G. Wagner, M. Baldini, M. Schmidbauer, K. Irmscher, R. Schewski, Z. Galazka, M. Albrecht, and R. Fornari, J. Crystal Growth **401**, 665 (2014).
[6]A. Kuramata, K. Koshi, S. Watanabe, Y. Yamaoka, T. Masui, and S. Yamakoshi, Jpn. J. Appl. Phys., Part 1 **55**, 1202A2 (2016).
[7]M. J. Tadjer, M. A. Mastro, N. A. Mahadik, M. Currie, V. D. Wheeler, J. A. Freitas, Jr., J. D. Greenlee, J. K. Hite, K. D. Hobart, C. R. Eddy, Jr., and F. J. Kub, J. Electron. Mater. **45**, 2031 (2016).
[8]S. Rafique, L. Han, M. J. Tadjer, J. A. Freitas, Jr., N. A. Mahadik, and H. Zhao, Appl. Phys. Lett. **108**, 182105 (2016).
[9]J. Kim, M. A. Mastro, M. J. Tadjer, and J. Kim, ACS Appl. Mater. Interfaces **9**, 21322 (2017).
[10]M. Higashiwaki, K. Sasaki, A. Kuramata, T. Masui, and S. Yamakoshi, Phys. Status Solidi A **211**, 21 (2014).
[11]M. J. Tadjer, N. A. Mahadik, V. D. Wheeler, E. R. Glaser, L. Ruppalt, A. D. Koehler, K. D. Hobart, C. R. Eddy, and F. J. Kub, ECS J. Solid State Sci. Technol. **5**, P468 (2016).
[12]A. J. Green, K. D. Chabak, E. R. Heller, R. C. Fitch, Jr., M. Baldini, A. Fiedler, K. Irmscher, G. Wagner, Z. Galazka, S. E. Tetlak, A. Crespo, K. Leedy, and G. H. Jessen, IEEE Electron Device Lett. **37**, 902 (2016).
[13]M. H. Wong, K. Sasaki, A. Kuramata, S. Yamakoshi, and M. Higashiwaki, IEEE Electron Device Lett. **37**, 212 (2016).
[14]S. Ahn, F. Ren, J. Kim, S. Oh, J. Kim, M. A. Mastro, and S. J. Pearton, Appl. Phys. Lett. **109**, 062102 (2016).
[15]J. B. Varley, J. R. Weber, A. Janotti, and C. G. Van de Walle, Appl. Phys. Lett. **97**, 142106 (2010).
[16]K. Irmscher, Z. Galazka, M. Pietsch, R. Uecker, and R. Fornari, J. Appl. Phys. **110**, 063720 (2011).
[17]Z. Zhang, E. Farzana, A. R. Arehart, and S. A. Ringel, Appl. Phys. Lett. **108**, 052105 (2016).
[18]E. Korhonen, F. Tuomisto, D. Gogova, G. Wagner, M. Baldini, Z. Galazka, R. Schewski, and M. Albrecht, Appl. Phys. Lett. **106**, 242103 (2015).
[19]B. E. Kananen, L. E. Halliburton, K. T. Stevens, G. K. Foundos, K. B. Chang, and N. C. Giles, Appl. Phys. Lett. **110**, 202104 (2017).
[20]P. Weiser, M. Stavola, W. Beall Fowler, Y. Qin, and S. Pearton, "Structure and vibrational properties of OH centers in β-Ga_2O_3" (to be published).
[21]J. Yang, F. Ren, S. J. Pearton, G. Yang, J. Kim, and A. Kuramata, J. Vac. Sci. Technol. B **35**, 031208 (2017).
[22]A. A. Arehart, E. Farzana, T. E. Blue, and S. A. Ringel, paper presented at 2nd International Workshop on Ga2O3 and Related Materials, Parma, Italy, September 2017.
[23]G. Yang, S. Jang, F. Ren, S. J. Pearton, and J. Kim, ACS Appl. Mater. Interfaces **9**, 40471 (2017).
[24]J. Yang, S. Ahn, F. Ren, S. J. Pearton, S. Jang, J. Kim, and A. Kuramata, Appl. Phys. Lett. **110**, 192101 (2017).
[25]L. Pautrat, B. Katircioglu, N. Magnea, D. Bensahel, J. C. Pfister, and L. Revoil, Solid-State Electron. **23**, 1159 (1980).
[26]G. M. Martin, A. Mitonneau, D. Pons, A. Mircea, and D. W. Woodard, J. Phys. C **13**, 3855 (1980).
[27]A. Y. Polyakov, N. B. Smirnov, I.-H. Lee, and S. J. Pearton, J. Vac. Sci. Technol. B **33**, 061203 (2015).
[28]I.-H. Lee, H.-S. Cho, K. B. Bae, A. Y. Polyakov, N. B. Smirnov, R. A. Zinovyev, J. H. Baek, T.-H. Chung, I. V. Shchemerov, E. S. Kondratyev, and S. J. Pearton, J. Appl. Phys. **121**, 045108 (2017).
[29]E. B. Yakimov, J. Alloys Compd. **627**, 344 (2015).
[30]I.-H. Lee, A. Y. Polyakov, E. B. Yakimov, N. B. Smirnov, I. V. Shchemerov, S. A. Tarelkin, S. I. Didenko, K. I. Tapero, R. A. Zinovyev, and S. J. Pearton, Appl. Phys. Lett. **110**, 112102 (2017).
[31]D. K. Schroeder, *Semiconductor Material and Device Characterization* (Wiley and Sons Inc., New York, 1990).
[32]J. B. Varley, A. Janotti, C. Franchini, and C. G. Van de Walle, Phys. Rev. B **85**, 081109 (2012).
[33]E. Chikoidze, A. Fellous, A. Perez-Tomas, G. Sauthier, T. Tchelidze, C. Ton-That, T. T. Huynh, M. Phillips, S. Russell, M. Jennings, B. Berini, F. Jomard, and Y. Dumont, Mater. Today Phys. **3**, 118 (2017).
[34]A. Armstrong, A. R. Arehart, D. Green, U. K. Mishra, J. S. Speck, and S. A. Ringel, J. Appl. Phys. **98**, 053704 (2005).
[35]A. M. Armstrong, M. H. Crawford, A. Jayawardena, A. Ahyi, and S. Dhar, J. Appl. Phys. **119**, 103102 (2016).